Structural and Multidisciplinary Optimization (2019) 60:965–981
https://doi.org/10.1007/s00158-019-02248-0

RESEARCH PAPER

A radial basis function-based multi-fidelity surrogate model: exploring correlation between high-fidelity and low-fidelity models

Xueguan Song[1] · Liye Lv[1] · Wei Sun[1] · Jie Zhang[2]

Received: 16 November 2018 / Revised: 28 January 2019 / Accepted: 22 February 2019 / Published online: 1 April 2019

Abstract

In computational simulation, a high-fidelity (HF) model is generally more accurate than a low-fidelity (LF) model, while the latter is generally more computationally efficient than the former. To take advantages of both HF and LF models, a multi-fidelity surrogate model based on radial basis function (MFS-RBF) is developed in this paper by combining HF and LF models. To determine the scaling factor between HF and LF models, a correlation matrix is augmented by further integrating LF responses. The scaling factor and relevant basis function weights are then calculated by employing corresponding HF responses. MFS-RBF is compared with Co-Kriging model, multi-fidelity surrogate based on linear regression (LR-MFS) model, CoRBF model, and three single-fidelity surrogates. The impact of key factors, such as the cost ratio of LF to HF models and different combinations of HF and LF samples, is also investigated. The results show that (i) MFS-RBF presents a better accuracy and robustness than the three benchmark MFS models and single-fidelity surrogates in about 90% cases of this paper; (ii) MFS-RBF is less sensitive to the correlation between HF and LF models than the three MFS models; (iii) by fixing the total computational cost, the cost ratio of LF to HF models is suggested to be less than 0.2, and 10–80% of the total cost should be used for LF samples; (iv) the MFS-RBF model is able to save an average of 50 to 70% computational cost if HF and LF models are highly correlated.

Keywords Multi-fidelity surrogate · Radial basis function · Correlation · Scaling factor · Robustness

1 Introduction

Design optimization relying on computational simulations, especially high-fidelity (HF) simulations, generally requires expensive computational cost (Wang and Shan 2006). To improve the computational efficiency, surrogate models have been used to replace computationally expensive simulations, which are constructed based on a small number of computational simulations. Surrogate models can be broadly classified into four types: single-fidelity, hybrid, adaptive sampling-based, and multi-fidelity surrogate models.

Single-fidelity surrogate models are the most conventional type and have been widely used in engineering applications. Popular single-fidelity surrogate models include the polynomial response surface (PRS) (Myers et al.2016), radial basis function (RBF) (Gutmann 2001; Sun et al. 2011), kriging (KRG) (Matheron 1963; Sacks et al. 1989), and support vector regression (SVR) (Smola and Schölkopf 2004). However, it has been shown that no single-fidelity surrogate model was found to be the most effective for all problems (Goel et al. 2007), and it is challenging to select the most appropriate single-fidelity surrogate prior.

Hybrid surrogate models ensemble multiple single-fidelity surrogate models by using weight coefficients. It is crucial to determine the weight coefficients for each single-fidelity surrogate model, and two types of method are generally used with constant or adaptive weights. It has been shown that hybrid surrogate models are able to take advantages of each single-fidelity surrogate model, thereby being more accurate and robust than individual surrogate models (Zerpa et al.

Responsible Editor: Raphael Haftka

✉ Liye Lv
lvhexiaoye@mail.dlut.edu.cn

Xueguan Song
sxg@dlut.edu.cn

Wei Sun
sunwei@dlut.edu.cn

Jie Zhang
jiezhang@utdallas.ed

[1] School of Mechanical Engineering, Dalian University of Technology, No.2 Linggong Road, Ganjingzi District, Dalian 116024, China

[2] Department of Mechanical Engineering, The University of Texas at Dallas, Richardson, TX 75080, USA

2005; Acar and Rais-Rohani 2009; Acar 2010; Liu et al. 2016).

Adaptive sampling-based surrogate models are proposed to enhance the accuracy by using auxiliary criteria called infilling strategies. Based on the strategy of choosing samples, infill strategies can be generally divided into two types: one-stage approach (e.g., goal seeking proposed by Jones (2001)) and two-stage approach (e.g., probability improvement (PI) proposed by Kushner (1964) and expected improvement (EI) presented by Schonlau et al. 1998). Theoretically, the accuracy of an adaptive sampling-based surrogate model could be improved gradually with the increase of infill points, but in reality, it often cannot be guaranteed as infill points can be misled if the initial surrogate significantly deviates from the true response (Jones 2001).

For the three types of surrogate models mentioned above, the observations at samples are usually obtained from HF simulations. However, it is still computationally expensive to run HF simulations despite of the advancement in computing power nowadays. To further reduce computational time and resources, multi-fidelity surrogate (MFS) models that fuse HF and low-fidelity (LF) information have been proposed by Kennedy and O'Hagan (2000) and subsequently investigated by Forrester et al. (2007), Han et al. (2013), Tyan et al. (2015), Cai et al. (2017a), etc. Kennedy and O'Hagan presented a Bayesian approach to improve surrogate modeling efficiency by fusing expensive and cheap simulations. Forrester et al. extended the KRG surrogate model to a CoKRG model, which can be used to find optimal solutions more quickly and enhance the accuracy of a surrogate model of the highest level of analysis. Han et al. modified an MFS model by using gradient information and showed that a gradient-enhanced CoKRG model was more efficient in aero-load prediction. Tyan et al. proposed a global variable-fidelity modeling method that makes it possible to build a global approximation of the scaling function using the design of experiments (DoE) and the RBF surrogate model. Cai et al. developed a multi-fidelity high-dimensional model representation method to tackle the risk of "curse of dimensionality."

In addition to KRG-based MFS models, other surrogate-based MFS models have also been developed in recent years. For example, Zhang et al. (2018) revised a heuristic MFS model based on linear regression (LR-MFS), to minimize prediction errors of HF samples. Cai et al. (2017b) proposed an adaptive MFS model based on RBF. Durantin et al. (2017) proposed a cooperative radial basis function (CoRBF) model, and compared the CoRBF model with CoKRG. Li et al. (2017) also developed a CoRBF model and found that it performed better than other baseline MFS models. Zhou et al. (2017a) transformed a multiple-to-one–dimensional structure to a one-to-one–dimensional structure by considering a LF model as prior knowledge. Zhou et al. (2017b) also proposed a sequential multi-fidelity model which aims at addressing an appreciate combination of HF and LF samples.

The hypothesis that a HF model is more accurate and more computationally expensive, whereas a LF model is less accurate but is considerably less computationally demanding (Viana et al. 2014), is generally assumed in the development of MFS methods. Thus, one of the key challenges in developing MFS models is how to optimally combine HF and LF information and take full advantage of the high accuracy of HF models and the high computational efficiency of LF models.

In this paper, a multi-fidelity surrogate model based on radial basis function (MFS-RBF) is developed. To construct the MFS-RBF model, an integrated correlation matrix between HF and LF samples is first constructed by augmenting the classical correlation matrix of an RBF model with LF responses. An integrated weight vector that consists of a scaling factor and relevant basis function weights are then calculated by employing HF responses. In the surrogate prediction process, an integrated correlation matrix is constructed between HF samples and testing points by augmenting LF responses at testing points. Instead of calculating LF responses directly, an RBF model built based on LF samples is used to approximate true LF responses. To evaluate the performance, MFS-RBF is compared with three baseline MFS models and three single-fidelity surrogate models on three numerical problems and one engineering problem. In addition, key factors that have significant influences on the accuracy of MFS-RBF are explored, such as the correlation between HF and LF models, the cost ratio of LF to HF models, the different combinations of HF and LF samples, the relationship between HF and LF sample set, and basis functions.

The remainder of this paper is organized as follows. Section 2 describes the overall framework of the developed MFS-RBF model. Comparisons between the MFS-RBF model and three baseline MFS models are presented in Section 3. Section 4 investigates the effects of key factors on the performance of MFS-RBF and computational cost savings. Conclusions and future works are provided in Section 5.

2 The MFS-RBF methodology

The MFS-RBF model is developed by integrating HF RBF surrogate model and LF RBF surrogate model through a scaling factor that is calculated based on a correlation matrix between HF and LF samples.

2.1 RBF surrogate model

A radial basis function (RBF) surrogate interpolates multivariate points (basis function centers) by using a series of symmetric basis functions. A typical form of RBF is expressed as:

$$\hat{y}(x) = \sum_{i=1}^{n} \lambda_i \phi(r(x, x_i)) \tag{1}$$

where $\hat{y}(x)$ is the prediction of a true response function, λ_i is the weighed coefficient for the i-th basis function, n is the number of samples, $r(x, x_i)$ denotes the Euclidean distance between the i-th sample x_i and a testing point x, and ϕ is a basis function. Basis functions usually include Gaussian (G), multi-quadric (MQ), and inverse multi-quadric (IMQ) functions, as summarized in Table 1.

Shape parameter σ shown in Table 1 can be determined in this paper by:

$$\sigma = d_{\max}/\sqrt{2n} \tag{2}$$

where n is the number of samples, and $d_{\max}$ is the maximum distance between any two samples.

To solve the unknown parameters λ_i, interpolation conditions can be used.

$$\hat{y}(x_i) = y(x_i), i = 1, 2, ..., n \tag{3}$$

By combining (1) and (3), a matrix form is given by:

$$\mathbf{\Phi\lambda} = \mathbf{y} \tag{4}$$

where $\mathbf{\Phi}$ is a correlation matrix, $\phi_{ik} = \phi(r(x_i - x_k))$, $k = 1, 2, ...n$.

2.2 MFS-RBF model

A typical form of an MFS model can be expressed as (5).

$$\mathbf{y_H}(\mathbf{x}) = \rho\mathbf{y_L}(\mathbf{x}) + \mathbf{d}(\mathbf{x}) \tag{5}$$

where $\mathbf{x}$ is a set of samples, $\mathbf{y_H}(\mathbf{x})$ and $\mathbf{y_L}(\mathbf{x})$ represent the responses of HF and LF models, respectively, ρ denotes a scaling factor, and $\mathbf{d}(\mathbf{x})$ is a discrepancy function between the HF and LF models. The construction of the MFS-RBF model consists of the following two steps.

2.2.1 Step 1: scaling factor determination

The samples of HF and LF models are represented as $\mathbf{x_H} = \{x_h^1, x_h^2, ..., x_h^n\}$ and $\mathbf{x_L} = \{x_l^1, x_l^2, ..., x_l^p\}$ ($\mathbf{x_H} \subset \mathbf{x_L}$), respectively. The corresponding responses of HF and LF models are denoted as $\mathbf{y_H} = \{y_h^1, y_h^2, ...y_h^n\}$ and $\mathbf{y_L} = \{y_l^1, y_l^2, ...y_l^p\}$, respectively. The HF and LF sample sets are denoted as ($\mathbf{x_H}$, $\mathbf{y_H}$) and ($\mathbf{x_L}$, $\mathbf{y_L}$), which include n and p samples, respectively. Equation (5) can be transformed to

$$\mathbf{y_H}(\mathbf{x_H}) = \rho\mathbf{y_L}(\mathbf{x_H}) + \mathbf{R}(\mathbf{x_H}, \mathbf{x_H})\boldsymbol{\omega} \tag{6}$$

Table 1 Typical basis functions in RBF

Name	Form
Gaussian function	$\phi(r) = e^{-r^2/\sigma^2}$
Multi-quadric function	$\phi(r) = \sqrt{r^2 + \sigma^2}$
Inverse multi-quadric function	$\phi(r) = 1/(r^2 + \sigma^2)$

where $\mathbf{y_H}(\mathbf{x_H})$ and $\mathbf{y_L}(\mathbf{x_H})$, respectively, represent the responses of HF and LF models at samples $\mathbf{x_H}$, ρ is a scaling factor, $\mathbf{R}(\mathbf{x_H}, \mathbf{x_H})$ is a correlation matrix between $\mathbf{x_H}$ and $\mathbf{x_H}$, and $\boldsymbol{\omega}$ is a vector of coefficients.

In the MFS-RBF model, the traditional correlation matrix $\mathbf{R}$ of an RBF model can be augmented as an integrated correlation matrix $\mathbf{C}$. Thereby, (6) can be written in a matrix form as

$$\mathbf{y_H} = \mathbf{C}\boldsymbol{\beta} \tag{7}$$

where $\mathbf{y_H}$ is a vector of HF responses; the integrated correlation matrix $\mathbf{C}$ is augmented by combining the LF responses at the HF samples and the correlation matrix of HF samples, i.e., $\mathbf{C}_{n\times(n+1)} = \begin{bmatrix} y_{lh}^1 & R(x_h^1, x_h^1) & ... & R(x_h^1, x_h^n) \\ ... & ... & ... & ... \\ y_{lh}^n & R(x_h^n, x_h^1) & ... & R(x_h^n, x_h^n) \end{bmatrix}$; $\boldsymbol{\beta}$ is an augmented coefficient vector constituted by ρ and $\boldsymbol{\omega}$, i.e., $\boldsymbol{\beta}_{(n+1)\times 1} = [\rho \ \omega_1 \ ... \ \omega_n]'$, where $[\omega_1 \quad ... \quad \omega_n]' = \boldsymbol{\omega}$.

In this paper, the rank of the matrix $\mathbf{C}$ is n, namely $\mathbf{C}$ is row full rank. According to the matrix theory (Petersen and Pedersen 2008), there exists unique least norm solution $\boldsymbol{\beta}$ indicating that MFS-RBF models can strictly go through HF samples. Then, the parameter vector $\boldsymbol{\beta}$ can be calculated by (8) which is transformed from (7), with obtained scaling factor ρ and $\boldsymbol{\omega}$. It is seen from (7) that the first element of $\boldsymbol{\beta}$ denotes the scaling factor ρ.

$$\boldsymbol{\beta} = \mathbf{C}^T\left(\mathbf{C}\mathbf{C}^T\right)^{-1}\mathbf{Y} \tag{8}$$

2.2.2 Step 2: prediction of MFS-RBF

The MFS-RBF model is finally formulated as.

$$\hat{\mathbf{y}}_{\mathbf{mf}}(\mathbf{x}) = \rho\hat{\mathbf{y}}_{\mathbf{L}}(\mathbf{x}) + \mathbf{r}(\mathbf{x}, \mathbf{x_L})\boldsymbol{\omega} \tag{9}$$

where $\hat{\mathbf{y}}_{\mathbf{mf}}(\mathbf{x})$ represents the vector of predictions calculated by MFS-RBF at testing points $\mathbf{x}$ (i.e., $\mathbf{x} = \{x_1, x_2, ..., x_m\}$, and m is the number of testing points); $\hat{\mathbf{y}}_{\mathbf{L}}(\mathbf{x})$ represents the vector of corresponding predictions of LF models; ρ and $\boldsymbol{\omega}$ can be obtained in Step 1; $\mathbf{r}(\mathbf{x}, \mathbf{x_L})$ is the correlation matrix between testing points $\mathbf{x}$ and LF samples $\mathbf{x_L}$. The matrix form is then formulated as

$$\hat{\mathbf{y}}_{\mathbf{mf}} = \mathbf{c}\boldsymbol{\beta} \tag{10}$$

where the integrated correlation matrix $\mathbf{c}$ is augmented by combining predictions of the LF model at testing points $\hat{\mathbf{y}}_{\mathbf{L}}(\mathbf{x})$ and the correlation matrix between LF samples and testing points $\mathbf{r}(\mathbf{x}, \mathbf{x_L})$, which is expressed as

$$\mathbf{c} = \begin{bmatrix} \hat{y}_l(x_1) & r(x_1, x_h^1) & ... & r(x_1, x_h^n) \\ ... & ... & ... & ... \\ \hat{y}_l(x_m) & r(x_m, x_h^1) & ... & r(x_m, x_h^n) \end{bmatrix} \tag{11}$$

The integrated correlation matrix **C** shown in (7) is augmented by adding LF responses at samples $\mathbf{x_H}$. Thus, in the prediction process, to construct the augmented matrix **c** between HF samples and testing points, corresponding responses of the LF model $\mathbf{y_L}(\mathbf{x})$ at testing points **x** are simultaneously needed. In addition to run LF simulations and get the LF sample set directly, an RBF model built based on the LF sample set ($\mathbf{x_L}$, $\mathbf{y_L}$) is used to obtain approximate responses $\hat{\mathbf{y}}_\mathbf{L}(\mathbf{x})$ at testing points **x**.

2.3 Performance criteria

Different metrics can be used to assess the modeling accuracy of MFS models, which can be broadly classified into two types, namely global criteria such as R^2 (i.e., *R*-square, coefficient of determination) and root mean square error (RMSE), local criteria such as relative maximum absolute error (RMAE). RMSE is highly correlated with R^2 and cannot express the goodness of fit intuitively, because the value of RMSE depends on responses. That is, for different problems, the value of RMSE varies with the responses. RMAE cannot represent the overall performance in the design space. Therefore, R^2 is selected as the only criterion for the comparisons in this paper.

In this paper, R^2 is adopted as the sole performance criterion, since RMSE is strongly correlated with R^2 and RMAE cannot reflect the global performance in the design space. The R^2 metric is calculated as

$$R^2 = 1 - \frac{\sum_{i=1}^{n}\left(y_i - \hat{y}_i\right)^2}{\sum_{i=1}^{n}\left(y_i - \overline{y}\right)^2} \tag{12}$$

where n is the number of samples; y_i and $\hat{y}_i$ represent true responses and predictions at testing points, respectively; and $\overline{y}$ is the means of true responses. Essentially, R^2 denotes the correlation between the true model and the surrogate model, and the surrogate model is more accurate if R^2 is closer to one.

The Pearson correlation coefficient (PCC), also referred to as *Pearson's r*, is a measure of the correlation between two random variables X and Y. In this paper, we use square of *Pearson's r* which is denoted as r^2 to describe the correlation between HF and LF functions which is inspired by Toal (2015), as shown in (13).

$$r^2 = \left(\frac{\sum_{i=1}^{n}\left(y_h - \overline{y}_h\right)\left(y_l - \overline{y}_l\right)}{\sqrt{\sum_{i=1}^{n}\left(y_h - \overline{y}_h\right)^2}\sqrt{\sum_{i=1}^{n}\left(y_l - \overline{y}_l\right)^2}} \right)^2 \tag{13}$$

where y_h and y_l denote the HF and LF responses, respectively; $\overline{y}_h$ and $\overline{y}_l$ represent the means of the HF and LF responses, respectively.

3 Numerical examples

3.1 Design of experiments

Design of experiments (DoEs) are methods to strategically generate samples from computer simulations or experiments in a domain of interest to build surrogate models. In this paper, it is assumed that the number of DoE (HF simulations) points is $m \times n$ for a single-fidelity surrogate model, where n is the dimension of the problem and m is a user-defined value. To build an MFS model, the number of HF samples is set to be $k \times n$ ($k < m$), and the remaining $(m-k) \times n$ HF simulations are replaced by more LF simulations. If the computational cost ratio between LF and HF models is θ, then the number of LF samples should be $(m-k) \times n/\theta$.

To evaluate the performance, the MFS-RBF model is compared with three benchmark MFS models (i.e., CoKRG (Forrester et al. 2007), LR-MFS (Zhang et al. 2018), and CoRBF (Durantin et al. 2017)) and three single-fidelity surrogate models (i.e., PRS, RBF-MQ, and KRG) through three widely used numerical test problems (i.e., the Forretal function ($n = 1$) from ref. Forrester et al. (2007), the Branin function ($n = 2$) from ref. Liu et al. (2016), and the Colville function ($n = 4$) from ref. Durantin et al. (2017)) and one engineering problem. It is worth noting that since the source code of the CoRBF model is not available, some specific parameters may be different from those in Durantin's paper even we wrote the code according to this paper. In addition, genetic algorithm (GA) is used for CoKRG and CoRBF models to search the unknown parameters, and for the LR-MFS model, a first-order PRS is used to approximate the discrepancy function. To determine the number of samples for building a surrogate, the accuracies of RBF-MQ with different sample sizes are compared. The criterion of $R^2 \geq 0.8$ is used to determine an appropriate sample size (Forrester et al. 2008). The accuracy is averaged over 50 randomly sampling sets.

In this paper, the standard Forretal, Branin, and Colville functions and the corresponding variants are considered as the HF and LF functions, respectively. In addition, the method of defining a LF function is inspired by Toal (2015), who introduced the thought of the correlation r^2 between HF and LF responses. For Forretal, Branin, and Colville cases, in Subsections 3.2, 3.3, and 3.4, the value of k is set as $0.8 \times m$, and then the numbers of HF samples for the Branin and Colville functions are 4, 8, and 32, respectively. The cost ratio θ is set to be 0.1, meaning that the computational cost of a HF model is 10 times of a LF model. Hence, the numbers of LF samples for the Branin and Colville functions are10, 20, and 80, respectively. For the engineering case in Subsection 3.4, the value of k is set as $0.5 \times m$, and then the numbers of HF samples are 5. The cost ratio θ is set to be 0.2, and then the number of LF samples is 25.

Among many available DoE methods, the Latin hypercube sampling (LHS) has been proved to be capable of balancing

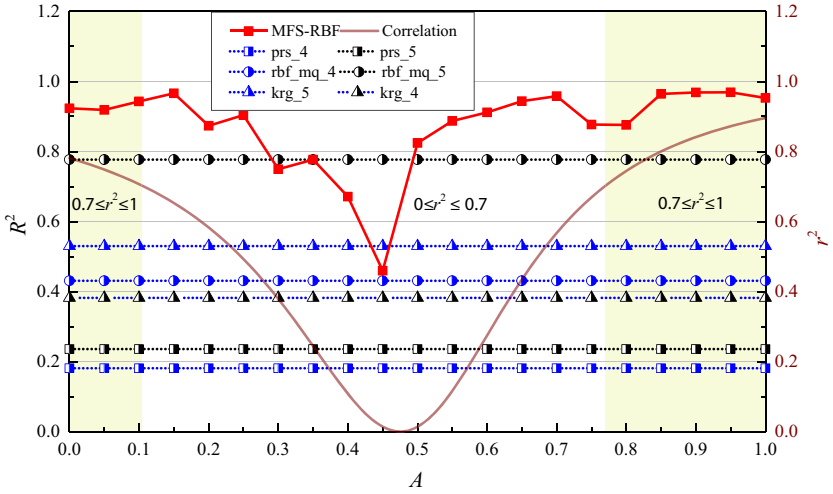

Fig. 1 Comparison between MFS-RBF and single-fidelity surrogate models for the Forretal function. "prs_4" means that the PRS model is constructed using 4*n* HF samples, as well as "rbf_mq_4" and "krg_4"; "prs_5" means that the PRS model is constructed using 5*n* HF samples, as well as "rbf_mq_5" and "krg_5"

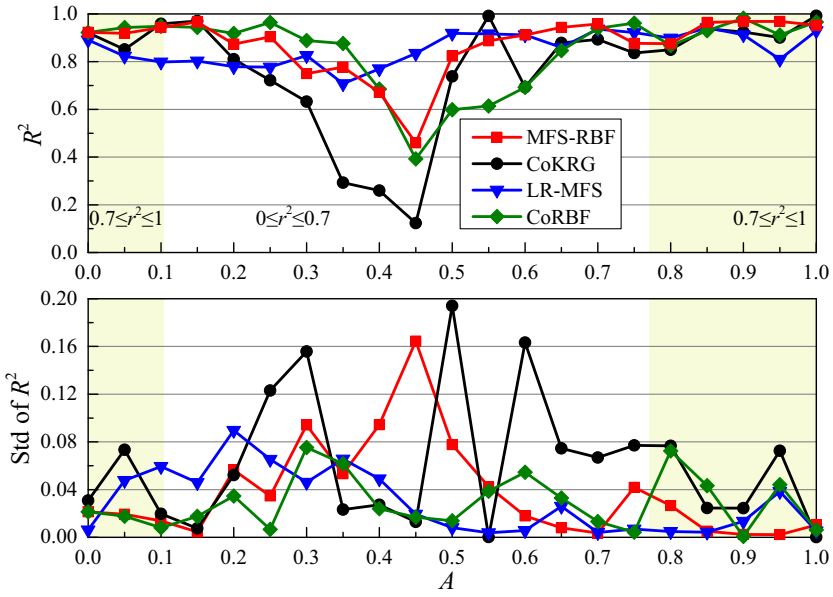

a) R^2 and Std of R^2 vary with the parameter A

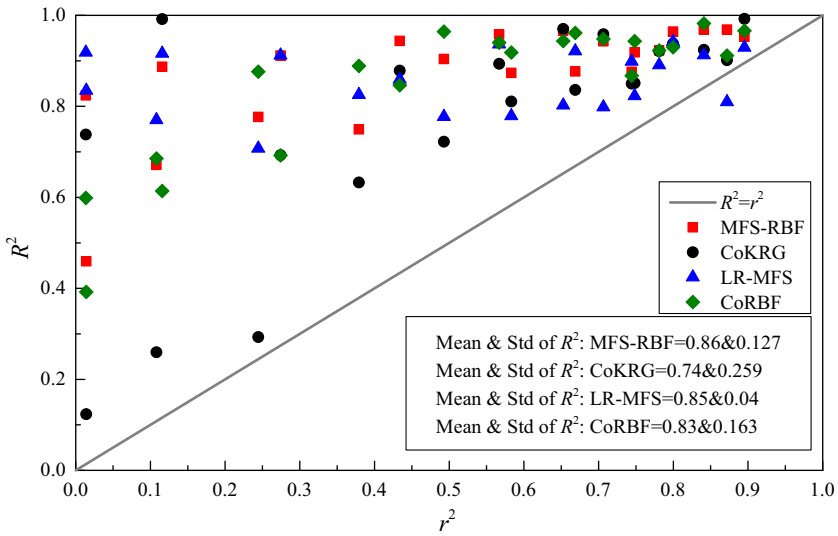

b) R^2 varies with the HF/LF correlation r^2

Fig. 2 Comparison of MFS models for the Forretal function. **a** R^2 and Std of R^2 vary with the parameter A. **b** R^2 varies with the HF/LF correlation r^2

the trade-off between accuracy and robustness by generating a near-random set of samples. For all surrogate models in this paper, the MATLAB function *lhsdesign* is adopted to generate DoE samples. To mitigate the impact of random DoE on surrogate performance, 20 sets of DoE samples are generated randomly and the averaged results are compared for the three numerical test problems. In addition, $1000 \times n$ randomly generated testing points are used for validation.

3.2 Test problem 1: Forretal function

In the case of Forretal function, to ensure that the correlation between HF and LF functions varies from 0 to 1, the LF function is derived from the HF function by multiplying a coefficient function of parameter A and adding a first-order term of x.

HF model:

$$y_h = (6x-2)^2 \sin(12x-4) \tag{14}$$

LF model:

$$y_l = \left(1-A^2-2A\right) y_h + 10(x-0.5)-5 \tag{15}$$

where $x \in [0, 1]$, y_h is a HF model, y_l is a LF model, and the parameter A varies from 0 to 1 to reflect the degree of the correlation r^2.

Figure 1 compares the MFS-RBF model with single-fidelity surrogate models. Two sample sets, $4n$ and $5n$, are generated to construct different single-fidelity surrogate models. To eliminate the effect of DoE, the accuracies of the single-fidelity surrogates are averaged over 20 randomly sampling sets. The red dashed line in Fig. 1 shows the relationship between correlation r^2 and the parameter A for the Branin function. It is observed that the MFS-RBF model with the minimum r^2 value is obtained when $A = 0.47$. The r^2 between the HF and LF models decreases as A increases from 0 to 0.47, while the r^2 increases as A increases from 0.47 to 1. A maximum r^2 is obtained when $A =$ 1. It is seen from Fig. 1 that the tendency for the performance of MFS-RBF strongly matches the tendency of the correlation r^2. From Fig. 1, we can see that MFS-RBF with $4n$ HF samples almost outperforms all single-fidelity surrogates no matter the sample number is $4n$ or $5n$.

Figure 2a compares the MFS-RBF, CoKRG, LR-MFS, and CoRBF models for the Forretal function on R^2 and the standard deviation (Std) of R^2. Each value of R^2 at parameter A is the average of the results obtained for 20 DoEs, and the Std of R^2 denotes the standard deviation of the 20 values. The results show that MFS-RBF performs better than CoKRG and is similar to CoRBF. It is interesting to find that the tendency of the performance of the MFS-RBF, CoKRG, and CoRBF models as shown in Fig. 2a is consistent with the tendency of the HF/LF model correlation r^2 as shown in Fig. 1, while the LR-MFS model is slightly insensitive to the correlation r^2.

Figure 2b shows the relationship between the HF/LF correlation r^2 and the accuracy R^2. It is observed that for the MFS-RBF, CoKRG, and CoRBF models, the accuracy R^2 increases as the correlation between the HF and LF models r^2 increases. This validates the assumption made in (5) in which a HF model can be represented as a function of a LF model. In addition, it is seen that the MFS-RBF model shows larger mean of R^2, which performs better than CoKRG and CoRBF models in terms of prediction accuracy and robustness.

3.3 Test problem 2: Branin function

Similar to the Forretal function, the LF function in Branin case is obtained from HF function by subtracting a quadratic term of x which multiplies a coefficient function of parameter A.

HF model:

$$y_h = \left(x_2 - \frac{5.1}{4\pi^2}x_1^2 + \frac{5}{\pi}x_1 - 6\right) + 10\left(1-\frac{1}{8\pi}\right)\cos(x_1) + 10 \tag{16}$$

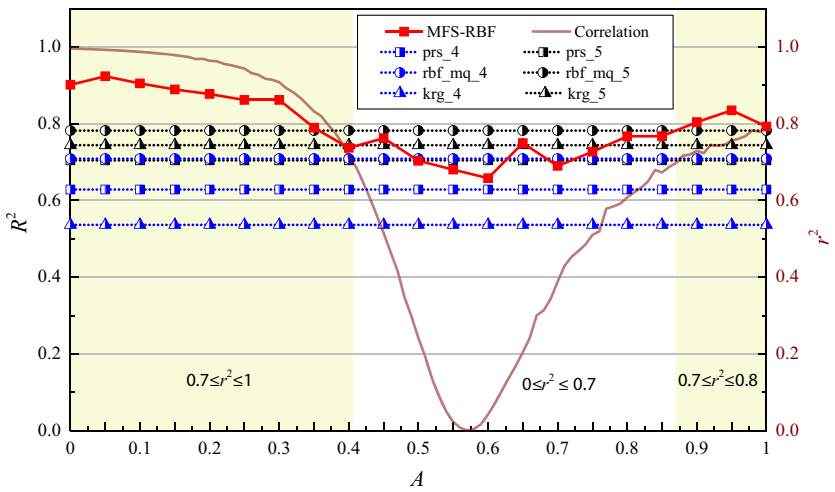

Fig. 3 Comparison between MFS-RBF and single-fidelity surrogate models for the Branin function

LF model:

$$y_l = y_h - (0.5A^2 + A + 0.2)\left(x_2 - \frac{5.1}{4\pi^2}x_1^2 + \frac{5}{\pi}x_1 - 6\right)^2 \quad (17)$$

where $x_i \in [-5, 10]$, x_i denotes the i-th variable for $i = 1, 2$.

Figure 3 compares the MFS-RBF model with single-fidelity surrogate models. Two sample sets, $4n$ and $5n$, are generated to construct different single-fidelity surrogate models. It is observed that the MFS-RBF model with the minimum r^2 value is obtained when $A = 0.57$. The r^2 between the HF and LF models decreases as A increases from 0 to 0.57, while the r^2 increases as A increases from 0.57 to 1. A maximum r^2 is obtained when $A = 0$. It is seen from Fig. 3 that the tendency for the performance of MFS-RBF strongly matches the tendency of the correlation r^2. When the correlation r^2 is greater than 0.8 (i.e., when $0 \le A \le 0.37$), MFS-RBF with $4n$ HF samples outperforms all single-fidelity surrogates no matter the sample number is $4n$ or $5n$. Overall, MFS-RBF performs better than the three single-fidelity surrogate models with fewer samples (i.e., "prs_4," "rbf_mq_4," and "krg_4") as A varies from 0 to 1.

Figure 4a compares the MFS-RBF, CoKRG, LR-MFS, and CoRBF models for the Branin function on the R^2 and Std of R^2. The results show that when A is less than 0.3, i.e., the

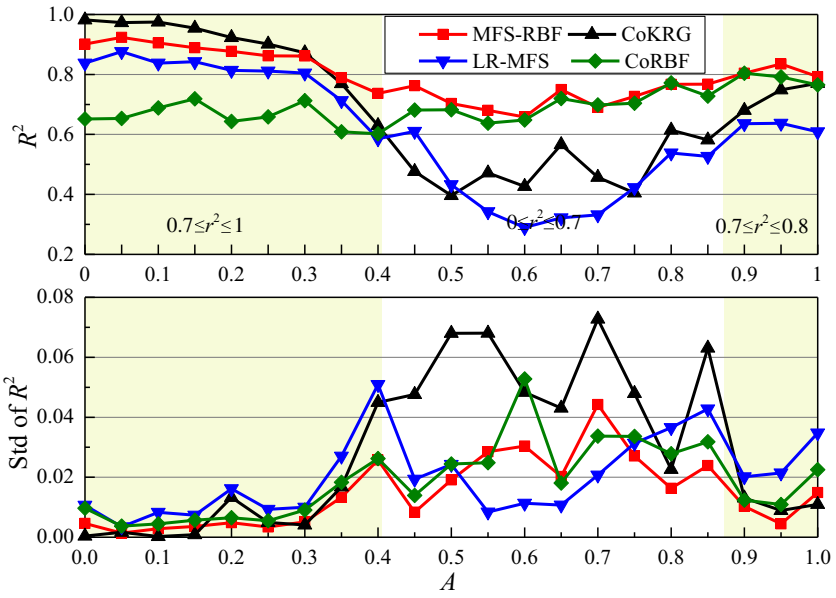

a) R^2 and Std of R^2 varies with the parameter A

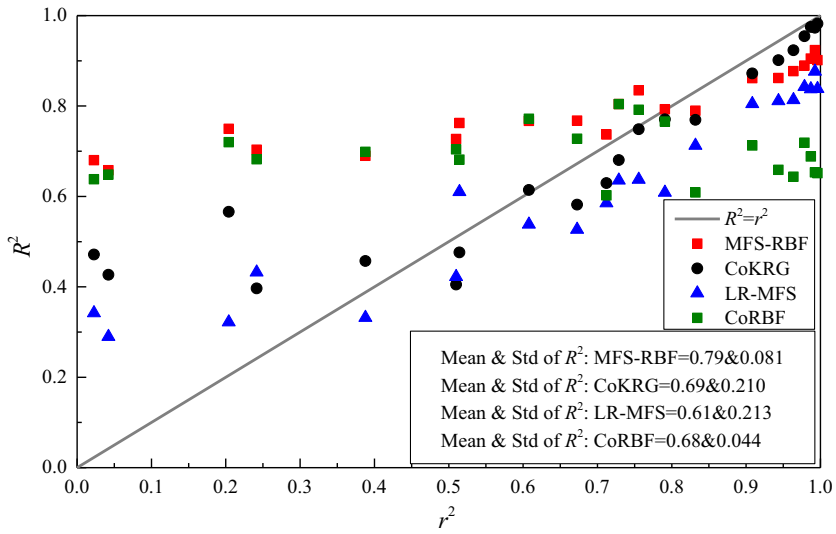

b) R^2 varies with the HF/LF correlation r^2

Fig. 4 Comparison of MFS models for the Branin function. **a** R^2 and Std of R^2 vary with the parameter A. **b** R^2 varies with the HF/LF correlation r^2

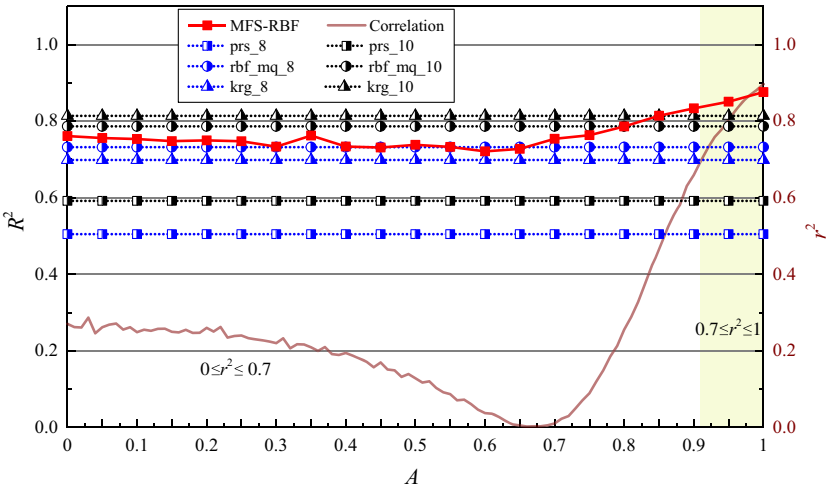

Fig. 5 Comparison between MFS-RBF and single-fidelity surrogate models for the Colville function. "prs_8" means that the PRS model is constructed using 8*n* HF samples, as well as "rbf_mq_8" and "krg_8"; "prs_10" means that the PRS model is constructed using 10*n* HF samples, as well as "rbf_mq_10" and "krg_10"

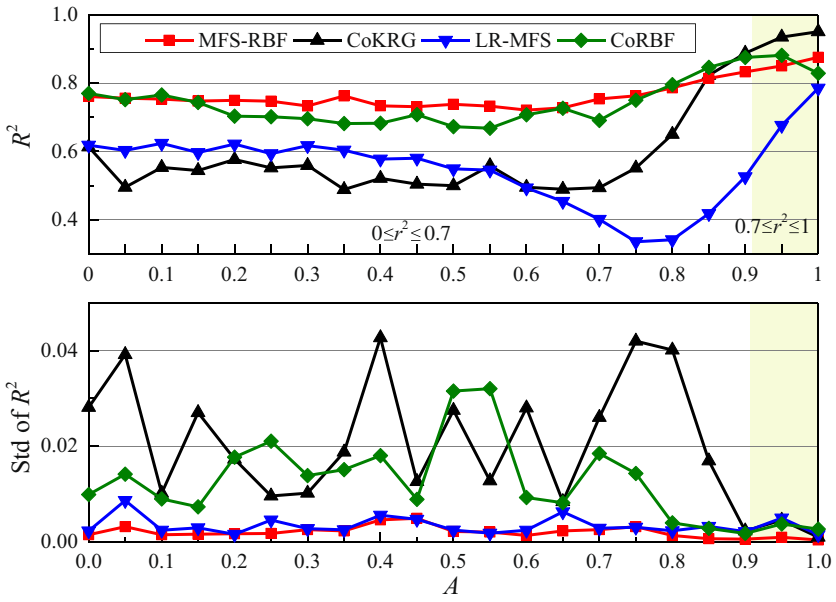

a) R^2 and Std R^2 of varies with the parameter A

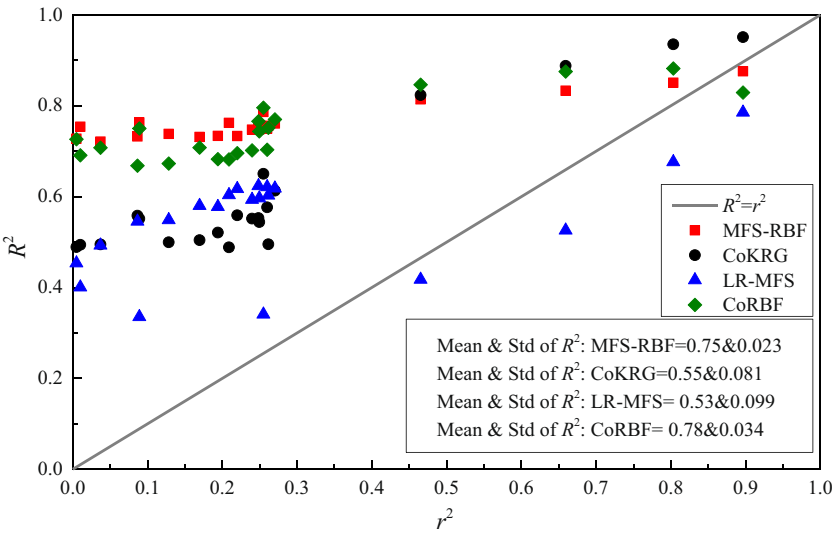

b) R^2 varies with the HF/LF correlation r^2

Fig. 6 Comparison of MFS models for the Colville function. **a** R^2 and Std of R^2 vary with the parameter A. **b** R^2 varies with the HF/LF correlation r^2

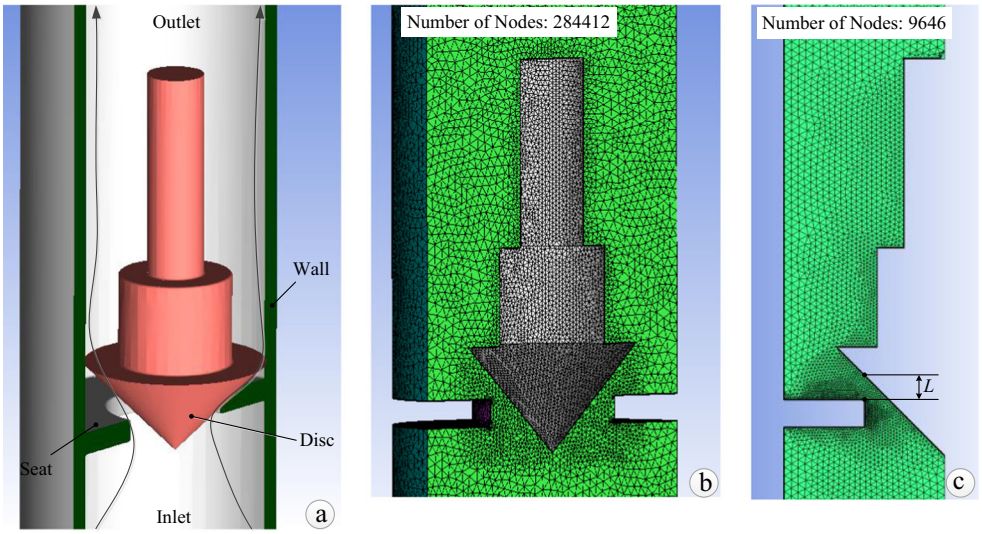

Fig. 7 Relief valve modeling. **a** Configuration. **b** 3-D CFD model. **c** 2-D CFD model

correlation r^2 is about 0.9, MFS-RBF performs worse than CoKRG but better than LR-MFS and CoRBF; when A is greater than 0.3, MFS-RBF outperforms all the MFS models in prediction accuracy. From the results of Std of R^2, we can see that MFS-RBF behaviors the best in terms of robustness as A varies from 0 to 1. It is also found that the tendency of the performance of the MFS-RBF, CoKRG, and LR-MFS models as shown in Fig. 4a is consistent with the tendency of the HF/LF model correlation r^2 as shown in Fig. 2.

Figure 4b shows the relationship between the HF/LF correlation r^2 and the accuracy R^2. It is observed that the accuracy R^2 increases as the correlation between the HF and LF models r^2 increases. This validates the assumption made in (5) in which a HF model can be represented as a function of a LF model. In addition, it is seen that the MFS-RBF model shows the largest mean of R^2, which outperforms the other three baseline MFS models in terms of prediction accuracy and robustness.

3.4 Test problem 3: Colville function

Similarly, for the case of the Colville function, the LF function is derived from the standard Colville function.

HF model:

$$y_h = 100\left(x_1^2 - x_2\right)^2 + (x_1 - 1)^2 + (x_3 - 1)^2 + 90\left(x_3^2 - x_4\right) + 10.1\left((x_2 - 1)^2 + (x_4 - 1)^2\right) + 19.8(x_2 - 1)(x_4 - 1) \quad (18)$$

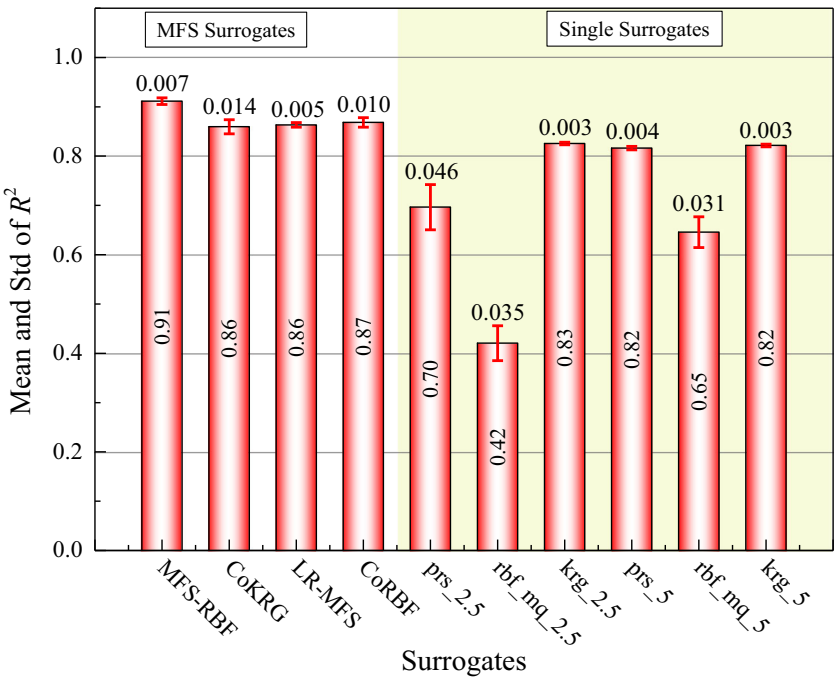

Fig. 8 Comparison of different MFS and single-fidelity models on the mean and Std of R^2. The legend of "prs_2.5" means that the PRS model is constructed using 2.5n HF samples, as well as "rbf_mq_2.5" and "krg_2.5"

Table 2 Sampling configurations for Branin and Colville

Cases		θ = 0.02	θ = 0.1	θ = 0.125	θ = 0.2	θ = 0.25
Branin (2-D)	HF	8	8	8	8	8
	LF	100	20	16	10	8
Colville (4-D)	HF	32	32	32	32	32
	LF	400	80	64	40	32

LF model:

$$y_l = y_h\left(A^2(x_1, x_2, x_3, x_4)\right) - (A + 0.5)\left(5x_1^2 + 4x_2^2 + 3x_3^2 + x_4^2\right) \quad (19)$$

where $x_i \in [-1, 1]$, x_i denotes the i-th variable for $i = 1, 2, 3, 4$.

Figure 5 compares the MFS-RBF model with single-fidelity surrogate models. Two sample sets, $8n$ and $10n$, are generated to construct different single-fidelity surrogate models. It is observed that the least r^2 occurs when $A = 0.68$. When $A \le 0.68$, r^2 monotonically decreases from 0.27 to 0. When $A \ge 0.68$, r^2 monotonically increases from 0 to 0.9. It is seen that the tendency of the MFS-RBF performance strongly matches the tendency of HF/LF correlation r^2. When the correlation r^2 is greater than 0.8, namely $A \ge 0.95$, MFS-RBF performs the best. When the correlation r^2 is less than 0.8, namely $0 \le A \le 0.95$, MFS-RBF always performs better than most single surrogate models except "rbf_mq_10" and "krg_10".

Figure 6a compares MFS-RBF, CoKRG, LR-MFS, and CoRBF based on R^2 and Std of R^2 for the Colville function. It is again found that the performance tendencies for all MFS models are consistent with the correlation tendency as shown in Fig. 5. In addition, MFS-RBF is relatively insensitive to the correlation r^2 than the other baseline MFS models and performs the best in robustness with the lowest Std of R^2. Figure 6b shows that the accuracy R^2 increases as the HF/LF correlation r^2 increases. Overall, the mean and Std of R^2 in Fig. 6 show that MFS-RBF outperforms the other three baseline MFS models in terms of robustness, and the accuracy performance of MFS-RBF is the best when the correlation is low.

3.5 Engineering problem

In addition to the three numerical problems, an engineering problem, i.e., computational fluid dynamic (CFD) analysis of a pressure relief valve (PRV) as shown in Fig. 7a, is conducted to investigate the performance of the developed MFS-RBF model. The flow enters the valve from the inlet, goes through the gap between the disc and the seat, and discharges from the outlet. The opening and closing of PRV are controlled by resultant force exerted on the disc. When the fluid force (F) is bigger than the force against on the disc, the PRV opens. To obtain the fluid force (F), steady simulations based on two CFD models with different dimensions are conducted. The standard $k-\varepsilon$ turbulent model is used; the medium is water with an initial temperature of 300 K. The three-dimensional (3-D) CFD model established using 284,412 unstructured grids (Fig. 7b) and the 2-D axisymmetric CFD model with 9646 unstructured grids (Fig. 7c) of the relief valve are considered as the HF and LF simulation models, respectively. In CFD simulations, the inlet pressure (P) is constant. The pressure of outlet is 0. The inlet pressure (P) and the opening lift (L) are selected as two design variables, with ranges of 0.1~0.4 atm and 1~4 mm, respectively (Fig. 7).

One HF simulation takes about 50 min, while one LF simulation takes about 10 min on a computer with a 3.4GHz processor and 8 cores CPU, and 16G RAM. Thus, the cost ratio θ of the LF model to the HF model is 0.2. To construct MFS models, each type of MFS model is constructed based on 5 ($2.5n$; n is the number of variables) HF samples and 25

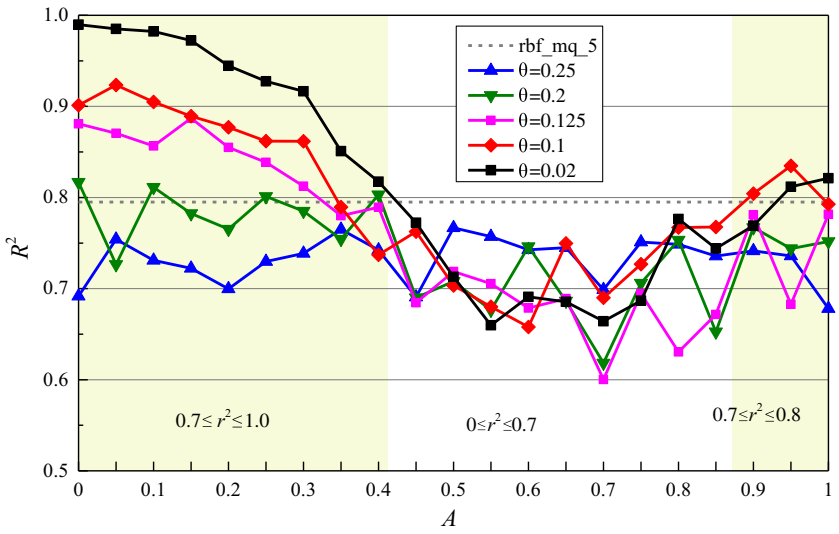

Fig. 9 The effect of the cost ratio on the performance of MFS-RBF for the Branin function

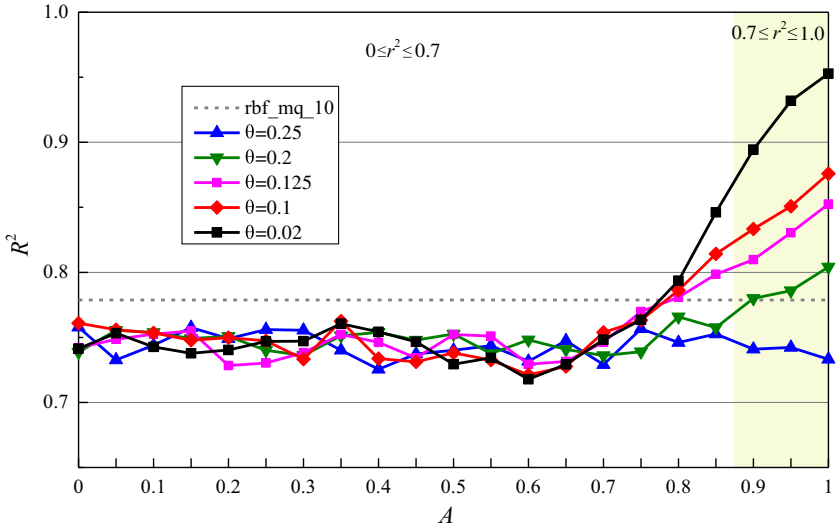

Fig. 10 The effect of the cost ratio on the performance of MFS-RBF for the Colville function

(12.5n) LF samples, and thus the total cost of constructing MFS models is equal to that of generating 10 (5n) HF samples. Another 40 randomly generated samples are used for validation. To eliminate the effect of DoE randomness, 20 sampling sets are generated and the results are averaged.

The comparison of MFS-RBF with three baseline MFS models and three single-fidelity surrogates are shown in Fig. 8. It is seen that MFS-RBF performs the best among all the surrogates for this engineering problem, as illustrated by the largest mean of R^2. Comparing with the other three MFS models, the MFS-RBF model also behaves better in the robustness metric with lower Std of R^2.

4 Exploring the effects of key MFS-RBF factors

In this section, we use Branin and Colville to further explore the effects of key factors on the performance of MFS-RBF. It is assumed that the total cost of generating DoE points is fixed, with a total budget of 5n and 10n HF samples for the Branin and Colville functions, respectively. All the results in this section are averaged over 20 random sampling sets to eliminate the effect of DoE.

4.1 Effect of the cost ratio of LF to HF models

It is assumed that the total cost of HF samples accounts for 4/5 of the total cost, and the remaining 1/5 is allocated to LF samples. That is, if the initial sample number is 5n ($m = 5$) and 10n ($m = 10$), 4n ($k = 4$) and 8n ($k = 8$) HF samples are used for the Branin and Colville functions, respectively. The remaining 1n ($m - k = 1$) and 2n ($m - k = 2$) HF samples are replaced by more LF samples ($(m - k)n/\theta$). To better evaluate the sensitivity of MFS to the cost ratio θ, five cost ratios of LF to HF models are compared in this subsection, i.e., 0.25, 0.2, 0.125, 0.1, and 0.02. The detailed sampling configurations according to different cost ratios for the Branin and Colville functions are summarized in Table 2.

Figure 9 illustrates the effect of different cost ratios on the performance of MFS-RBF for the Branin function. It is observed that when the cost ratio θ decreases, the performance of MFS-RBF becomes more sensitive to the correlation r^2, the accuracy of MFS-RBF is improved significantly (as shown by the mean of R^2), and the robustness of MFS-RBF is slightly improved except in the case of $\theta = 0.25$ (as shown by the Std of R^2). It is seen from Fig. 9 that MFS-RBF with $\theta = 0.25$ shows the worst performance as illustrated by the lowest R^2 at most time. The HF/LF correlation r^2 shows little influence on the performance of MFS-RBF when $\theta = 0.25$ and $\theta = 0.2$. Thus, the MFS-RBF model may not be suitable for the condition that the cost ratio $\theta \ge 0.2$.

It is seen from Fig. 9 that when the correlation r^2 is greater than 0.7, MFS-RBF shows the best accuracy and robustness in the case of $\theta = 0.02$. When the correlation $0 \le r^2 \le 0.7$, the performance of MFS-RBF with $\theta = 0.25$ performs the best but is still poor as shown by small values of R^2. The variation in the robustness is partially due to that more LF samples are added in the MFS-RBF model when decreasing the cost ratio θ, thereby more LF information is blended into MFS-RBF. Thus, the accuracy of the LF model also significantly affects the MFS-RBF model. When the HF/LF correlation r^2 is

Table 3 Sampling configurations for Branin and Colville

Cases		1_4	2_3	2.5_2.5	3_2	4_1	4.5_0.5
Branin (2-D)	HF	2	4	5	6	8	9
	LF	80	60	50	40	20	10
Colville (4-D)	HF	8	16	20	24	32	36
	LF	320	240	200	160	80	40

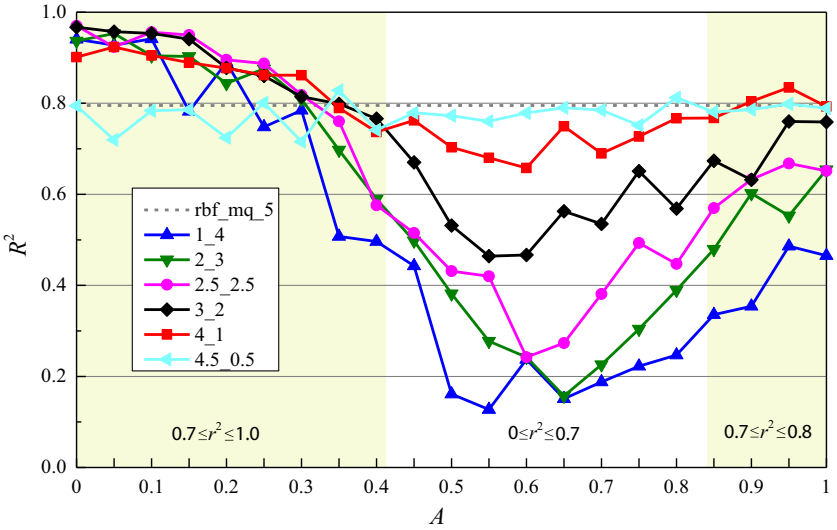

Fig. 11 Impact of the combination of HF and LF samples on the performance of MFS-RBF for Branin

strong, it has positive impact on the performance of MFS-RBF, while when the HF/LF correlation r^2 is weak, it has negative impact on the performance of MFS-RBF.

Figure 10 illustrates the effect of different cost ratios on the performance of MFS-RBF for the Colville function as A changes from 0 to 1. It is seen from Fig. 10 that when $r^2 \geq 0.7$, the performance of MFS-RBF becomes more sensitive to the HF/LF correlation with the increase of cost ratio θ, which is similar to the results observed for the Branin function.

From Fig. 10, we observe that when the correlation r^2 is less than 0.7, cost ratio θ has no significant influence on the performance of MFS-RBF. When the correlation r^2 is greater than 0.7, the performance of MFS-RBF becomes better as the cost ratio θ decreases. In this case, the LF and HF models are more correlated. A lower cost ratio θ indicates a larger size of LF samples, and the LF model can be fitted more accurately. A relatively more accurate LF model can improve the performance of MFS-RBF when HF and LF models have strong correlation.

4.2 Effect of the different combinations of HF and LF samples

To better explore the effect of different combinations of HF and LF samples, the cost ratio θ is set to be 0.1. The total cost used to generate HF samples for single-fidelity surrogates is divided into six cases, namely "1_4," "2_3," "2.5_2.5," "3_2," "4_1," and "4.5_0.5." For the Branin (or Colville) function, the case of "1_4" means that the cost of running $1/5 \times 5n$ (or $1/5 \times 10n$) HF samples is allocated to generate HF samples, and the cost of running $4/5 \times 5n$ (or $4/5 \times 10n$) HF samples is allocated to generate LF samples, as well as other cases. The detailed sampling configurations according to different combinations of HF and LF samples for Branin and Colville are summarized in Table 3.

Figure 11 illustrates the effect of different combinations of HF and LF samples on the performance of MFS-RBF for the Branin function. By comparing Fig. 11 with Fig. 1, it is

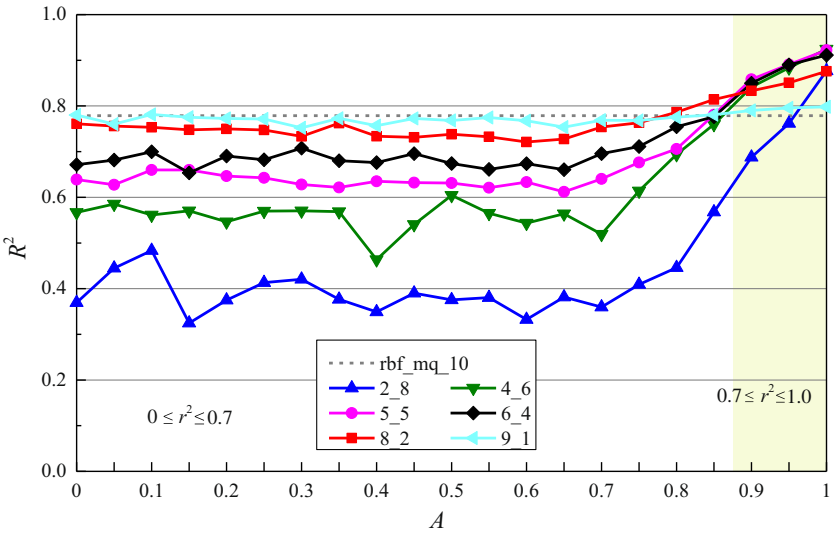

Fig. 12 Impact of the combination of HF and LF samples on the performance of MFS-RBF for Colville

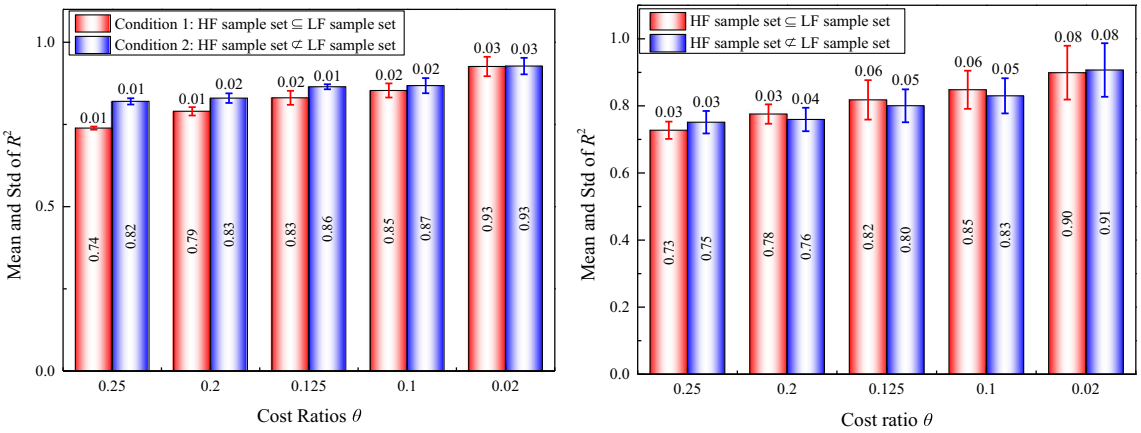

a) Branin function b) Colville function

Fig. 13 Comparison of different cost ratios when $r^2 \geq 0.7$. **a** Branin function. **b** Colville function

observed that MFS-RBF with more HF samples and fewer LF samples (e.g., cases "4_1" and "4.5_0.5") is less sensitive to the correlation r^2. This can be attributed to the less biased information (from the LF samples) integrated into MFS-RBF. MFS-RBF tends to be more robust when increasing the number of HF samples. Regarding the prediction performance, when the correlation r^2 is less than 0.7, MFS-RBF performs better with increase of the HF sample size, but always behaves worse than the single-fidelity RBF model constructed from $5n$ HF samples; when the correlation r^2 is greater than 0.7, MFS-RBF in the cases of "3_2" and "2.5_2.5" has a slightly better performance than that of in the cases of "4_1," "2_3," and "1_4." In addition, the MFS-RBF model in the case of "4.5_0.5" still performs worse than the single-fidelity surrogate "rbf_mq_5."

Figure 12 illustrates the effect of different combinations of HF and LF samples on the performance of MFS-RBF for the Colville function as A varies from 0 to 1. The results of the Colville function are similar to those of the Branin function. When the correlation r^2 is less than 0.7, it is observed that the accuracy of MFS-RBF with more HF samples is improved but still worse than the single-fidelity surrogate model "rbf_mq_10"; when the correlation r^2 is greater than 0.7, the MFS-RBF with more HF samples performs worse (e.g., case "4.5_0.5") than those with fewer HF samples (e.g., case "4_1"). By comparing Fig. 10 and Fig. 3, the MFS-RBF model becomes less sensitive to the correlation r^2 by adding more HF samples. The case "1_4" always performs the worst as the correlation r^2 increases. Thus, it is suggested that 10–80% of the total budget should be used for generating LF samples.

4.3 Effect of the relationship between HF and LF samples

In the Subsections 4.1 and 4.2, it is assumed that the HF sample set is a subset of the LF sample set which is denoted by "Condition 1." In this part, the performance of the MFS-BRF model is investigated when the HF sample set is *not* a subset of the LF sample set which is expressed by "Condition 2." The

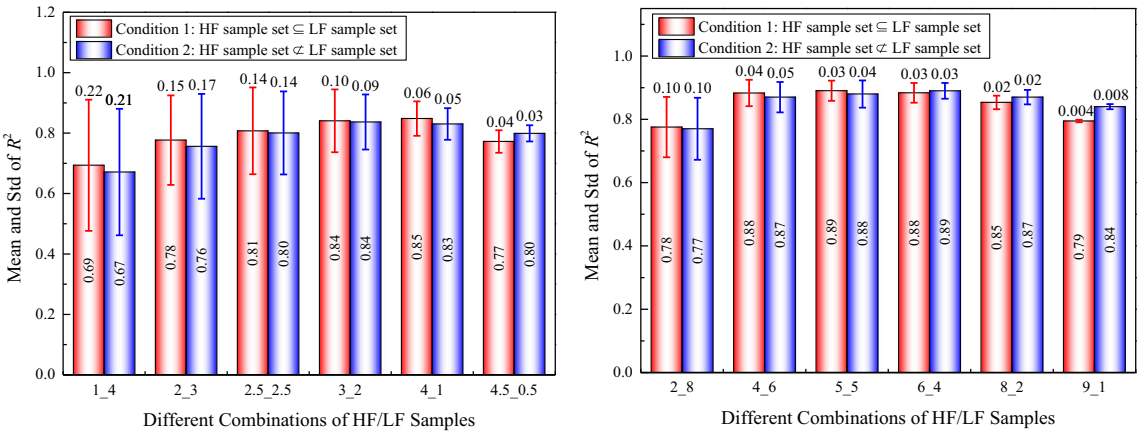

a) Branin function b) Colville function

Fig. 14 Comparison of different combinations of HF and LF samples when $r^2 \geq 0.7$. **a** Branin function. **b** Colville

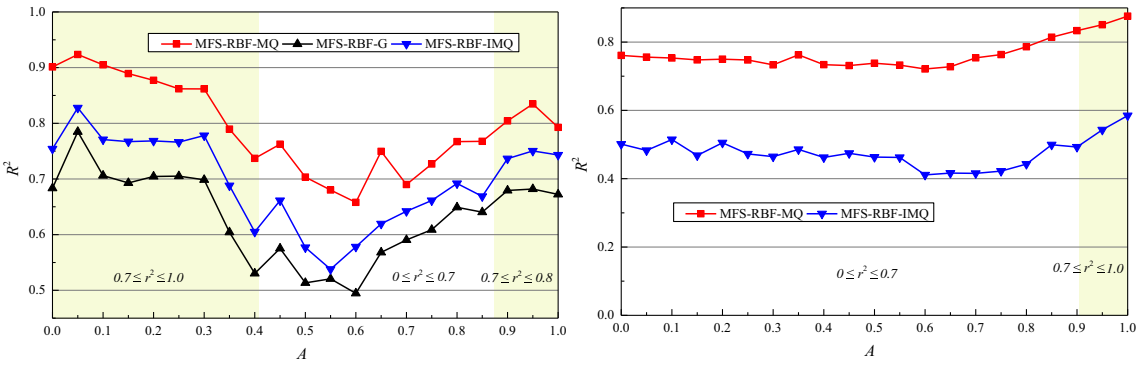

Fig. 15 Effect of different basis functions on the performance of MFS-RBF model. **a** Branin function. **b** Colville function

relevant settings, such as sample size, correlations, and combinations in this part, are the same as those in Subsections 4.1 and 4.2. Figures 13 and 14 show the comparisons of different cost ratios and combination of HF and LF samples on the performance of MFS-RBF through the Branin and Colville functions. The blue columns express the mean and Std of R^2 when $r^2 \geq 0.7$ in the case of "Condition 2," while the red columns denote the mean and Std of R^2 when $r^2 \geq 0.7$ obtained in the case of "Condition 1" in Subsections 4.1 and 4.2.

From Figs. 13 and 14, accuracy and robustness metrics in terms of "Condition 2" are consistent with those in the case of "Condition 1" for the Branin and Colville functions. Overall, it can be concluded that HF sample set is not necessarily a subset of LF sample set. It is worth noting that the HF sample set is still a subset of the LF sample set in the rest of this paper.

4.4 Effect of the different basis functions

In this subsection, the effect of different basis functions of MFS-RBF models is explored. For the Branin (Colville) function, the total budget is the cost of 5*n* (10n) HF samples and the number of HF samples is 4*n* (8*n*). The cost ratio θ is set to be 0.1. Basis functions used in this part are shown in Table 1, including multi-quadric (MQ), Gaussian (G), and inverse multi-quadric (IMQ) functions. Figure 15 shows that in terms of accuracy and robustness, MFS-RBF with MQ basis function performs the best, MFS-RBF with IMQ basis function behaves the second, and MFS-RBF with G basis function is the worst. From Fig. 15b, we can see that when the basis function is G, R^2 has no results, which means that the accuracy of the MFS-BRF with G basis function is too poor. Overall, MFS-RBF with MQ basis function behaves the best, and MQ is suggested to be chosen as the basis function of the MFS-RBF model in this paper.

4.5 Computational cost

In addition to the accuracy improvement, this subsection further investigates computational cost savings from the MFS-RBF model. It is assumed that the cost ratio of LF to HF functions θ is 0.1 and the MFS-RBF model is constructed with the "4_1"

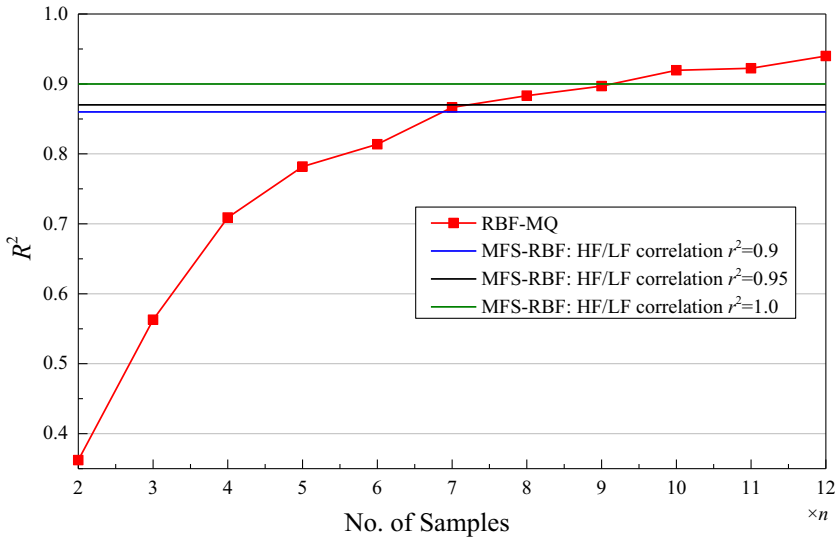

Fig. 16 Computational cost of MFS-RBF and RBF-MQ under different correlation values for Branin

Table 4 Computational cost of MFS-RBF and RBF-MQ under different correlation values for Branin

Correlation r^2	MFS-RBF cost	Accuracy R^2	RBF cost	Cost saving
0.9	$5n$	0.86	$\sim 7n$	40%
0.95	$5n$	0.87	$7n$	40%
1.0	$5n$	0.90	$9n$	80%

Table 5 Computational cost of MFS-RBF and RBF-MQ under different correlation values for Colville

Correlation r^2	MFS-RBF cost	Accuracy R^2	RBF cost	Cost save
0.8	$10n$	0.85	$\sim 15n$	50%
0.9	$10n$	0.88	$\sim 19n$	90%

combination as defined above. It is seen that MFS-RBF performs relatively better when $r^2 \geq 0.7$, and hence the computational cost comparison is performed under large correlation r^2 values in this subsection. In addition, since the MFS-RBF model is an RBF-MQ-based multi-fidelity surrogate model, we compare the MFS-RBF model to a single-fidelity RBF-MQ model.

For the Branin function, the comparisons are implemented under three HF/LF correlation values, namely $r^2 = 0.9$, $r^2 = 0.95$, and $r^2 = 1.0$. In these three cases, the total computational cost of MFS-RBF models is the same, with the total budget of $5n$ HF models. Figure 16 and Table 4 show the computational cost of MFS-RBF and RBF-MQ under the three correlation cases. It is seen from Fig. 16 that when the correlation $r^2 = 0.9$, the R^2 of MFS-RBF built from $5n$ samples is approximately 0.86, which is similar to the RBF-MQ when using the same number of $7n$ samples, and then MFS-RBF saves approximately 40% computational cost. When the correlation $r^2 = 0.95$, the R^2 of MFS-RBF is approximately 0.87, and RBF-MQ requires more than $7n$ samples to attain the same accuracy. Hence, MFS-RBF saves approximately 40% computational cost. When the correlation $r^2 = 1.0$, the R^2 of the MFS-RBF model is about 0.90, and RBF-MQ requires $9n$ samples to attain the same accuracy. Hence, MFS-RBF saves approximately 80% computational cost. Overall, MFS-RBF saves an average of 50% computational cost.

For the Colville function, the comparisons are implemented under two correlation values, namely $r^2 = 0.8$ and $r^2 = 0.9$. In these two cases, the total computational cost of MFS-RBF models is the same, with the total budget of $10n$ HF models. Figure 17 and Table 5 show the computational cost of MFS-RBF and RBF-MQ under the two correlation cases.

From Fig. 12, we observe that when the correlation $r^2 = 0.8$, the R^2 of MFS-RBF built by $10n$ samples is about 0.85, and RBF-MQ model requires about $15n$ samples to attain the same accuracy. Thereby, MFS-RBF saves approximately 50% computational cost compare with single RBF surrogate. When the correlation $r^2 = 0.9$, the R^2 of the MFS-RBF model is about 0.88, and RBF-MQ model requires $19n$ samples to attain the same accuracy. Hence, the MFS-RBF model saves approximately 90% computational cost. Overall, the MFS-RBF model saves an average of 70% computational cost.

5 Conclusions

A multi-fidelity surrogate model based on RBF, called MFS-RBF, was developed in this paper. MFS-RBF integrated high-fidelity and low-fidelity models by using a scaling factor and an augmented correlation matrix. To validate the performance of MFS-RBF, three benchmark MFS models (i.e., CoKRG, LR-MFS, and CoRBF) and three widely used single-fidelity surrogates (i.e., PRS, RBF-MQ, and KRG) were selected, and three numerical test problems and one engineering problem under different correlations between HF and LF models were tested. Comparison results showed that when the correlation

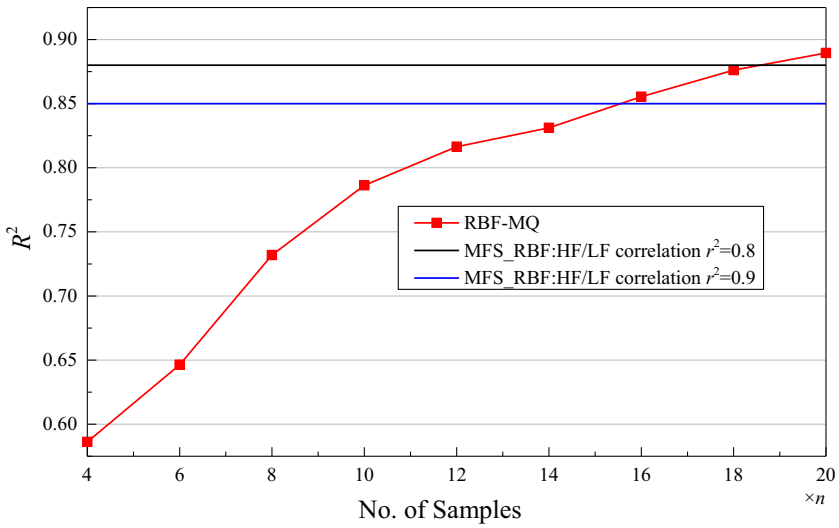

Fig. 17 Computational cost of MFS-RBF and RBF-MQ under different correlation values for Colville

r^2 between HF and LF models is greater than 0.7, MFS-RBF generally performs better than single-fidelity surrogates. MFS-RBF also performed better than three baseline MFS models in terms of both accuracy and robustness. The results of this paper will be of great help for the MFS research community, for example, to strengthen the understanding whether a MFS model could be trusted, and to provide suggestion under what conditions a MFS model would be better than a single surrogate model.

The effects of key factors on the performance of MFS models were also investigated, including the cost ratio θ, the combination of HF and LF samples, the relationship between HF and LF samples, and basis functions. Results showed that MFS-RBF is less sensitive to the correlation between HF and LF models than the three baseline MFS models. This finding is more useful for real engineering applications, as the correlation between HF and LF models is generally unknown prior and could be weak in many cases. It was also found that with the same total computational cost, (i) the cost ratio of LF to HF is suggested to be less than 0.2, (ii) 10–80% of the total cost should be used for generating LF samples, (iii) the HF sample set is not necessarily to be a subset of LF sample set, and (iv) a MFS-RBF model with the MQ basis function performs the best. The computational cost of MFS-RBF was also investigated, and the results showed that MFS-RBF could save an average of 50 to 70% computational cost when HF and LF models are strongly correlated.

In this paper, we assumed that the cost ratio θ and the correlation r^2 are independent, but this is not always true in practice. In a situation such as the LF model is a coarser 3-D model and the HF model is a finer 3-D model, the cost ratio θ and the correlation are dependent. Future work will model the coupling effects between the cost ratio and the correlation to further improve MFS-RBF.

Funding information The research is supported by the National Natural Science Foundation of China (Grant No. 51505061 and Grant U1608256).

Compliance with ethical standards

Conflict of interest statement The authors declare that they have no conflict of interest.

Replication of results The main codes and raw data corresponding to each figure are submitted as supplementary materials.

References

Acar E (2010) Various approaches for constructing an ensemble of metamodels using local measures. Struct Multidiscip Optim 42(6): 879–896

Acar E, Rais-Rohani M (2009) Ensemble of metamodels with optimized weight factors. Struct Multidiscip Optim 37(3):279–294

Cai X, Qiu H, Gao L, Shao X (2017a) Metamodeling for high dimensional design problems by multi-fidelity simulations. Struct Multidiscip Optim 56(1):151–166

Cai X, Qiu H, Gao L, Wei L, Shao X (2017b) Adaptive radial-basis-function-based multifidelity metamodeling for expensive black-box problems. AIAA J 55(7):1–13

Durantin C, Rouxel J, Désidéri JA, Glière A (2017) Multifidelity surrogate modeling based on radial basis functions. Struct Multidiscip Optim 56(5):1061–1075

Forrester AIJ, Sóbester A, Keane AJ (2007) Multi-fidelity optimization via surrogate modelling. Proceedings of the royal society a: mathematical, physical and engineering sciences 463(2088):3251–3269

Forrester AIJ, Sóbester A, Keane AJ (2008) Engineering design via surrogate modelling: a practical guide. DBLP, Trier

Goel T, Haftka RT, Wei S, Queipo NV (2007) Ensemble of surrogates. Struct Multidiscip Optim 33(3):199–216

Gutmann HM (2001) A radial basis function method for global optimization. J Glob Optim 19(3):201–227

Han ZH, Görtz S, Zimmermann R (2013) Improving variable-fidelity surrogate modeling via gradient-enhanced kriging and a generalized hybrid bridge function. Aerosp Sci Technol 25(1):177–189

Jones DR (2001) A taxonomy of global optimization methods based on response surfaces. J Glob Optim 21(4):345–383

Kennedy MC, O'Hagan A (2000) Predicting the output from a complex computer code when fast approximations are available. Biometrika 87(1):1–13

Kushner HJ (1964) A new method of locating the maximum point of an arbitrary multipeak curve in the presence of noise. J Basic Eng 86(1): 97–106

Li X, Gao W, Gu L, Gong C, Jing Z, Su H (2017) A cooperative radial basis function method for variable-fidelity surrogate modeling. Struct Multidiscip Optim 56(5):1077–1092

Liu H, Xu S, Wang X, Meng J, Yang S (2016) Optimal weighted pointwise ensemble of radial basis functions with different basis functions. AIAA J 54(10):1–17

Matheron G (1963) Principles of geostatistics. Econ Geol 58(8):1246–1266

Myers RH, Montgomery DC, Anderson-Cook, CM (2016) Response surface methodology: process and product optimization using designed experiments. J. Wiley & Sons

Petersen KB, Pedersen MS (2008) The matrix cookbook. Technical University of Denmark 7(15):510

Sacks J, Welch WJ, Mitchell TJ, Wynn HP (1989) Design and analysis of computer experiments. Stat Sci 4(4):409–423

Schonlau M, Welch WJ, Jones DR (1998) Global versus local search in constrained optimization of computer models. Lecture Notes-Monograph Series 34:11–25

Smola AJ, Schölkopf B (2004) A tutorial on support vector regression. Stat Comp 14(3): 199–222

Sun G, Li G, Gong Z, He G, Li Q (2011) Radial basis functional model for multi-objective sheet metal forming optimization. Eng Optim 43(12):1351–1366

Toal DJJ (2015) Some considerations regarding the use of multi-fidelity Kriging in the construction of surrogate models. Struct Multidiscip Optim 51(6): 1223–1245

Tyan M, Nguyen NV, Lee JW (2015) Improving variable-fidelity modelling by exploring global design space and radial basis function networks for aerofoil design. Eng Optim 47(7):885–908

Viana FAC, Simpson TW, Balabanov V, Toropov V (2014) Special section on multidisciplinary design optimization: metamodeling in multidisciplinary design optimization: how far have we really come? AIAA J 52(4):670–690

Wang GG, Shan S (2006) Review of metamodeling techniques in support of engineering design optimization. ASME 2006 international design engineering technical conferences and computers and information in engineering conference. Am Soc Mech Eng 129(4):415–426

Zerpa LE, Queipo NV, Pintos S, Salager JL (2005) An optimization methodology of alkaline–surfactant–polymer flooding processes using field scale numerical simulation and multiple surrogates. J Pet Sci Eng 47(3):197–208

Zhang Y, Kim NH, Park C, Haftka RT (2018) Multifidelity surrogate based on single linear regression. AIAA Journal, 56(12) 4944–4952

Zhou Q, Jiang P, Shao X, Hu J, Cao L, Wan L (2017a) A variable fidelity information fusion method based on radial basis function. Adv Eng Inform 32(C):26–39

Zhou Q, Wang Y, Choi SK, Jiang P, Shao X, Hu J (2017b) A sequential multi-fidelity metamodeling approach for data regression. Knowl-Based Syst 134:199–212